Numerical simulation of Penning gas discharge in 2D/3D setting

A. Rokhmanenkov[1], S. Kuratov[1]

[1] *Dukhov Research Institute of Automatics (FSUE VNIIA), Moscow, Russia*

In [1] classical Penning gas discharge has been studied. Cylindrical anode is placed between two circular cathodes with small gaps (relative to the size of anode) between cathode and anode (figure 1). Experimental parameters relevant for the numerical simulation are given in the [1]. External magnetic field is produced by electric coil.

External magnetic field in the system iscreated by an electromagnetic coil [1]. This allowed varying the magnetic induction in the range of 200÷500 G. In the experiments molecular hydrogen was used [1]. The pressure of the gas was varied in the range of 0.8÷1.0 $mTorr$. Anode potential was changed in the range 600÷800 V. In the experiments [1] dependence of the discharge current on the magnetic induction was measured (figure 2). It can be seen that as the magnetic field increased from 200 G to 300 G, the discharge current increased. When the magnetic field was about 300-350 G, there was some fluctuation of the discharge current. And with an increased in the magnetic field above 350 G, the discharge current decreased. It turns out that there is some optimal value of the magnetic field at which the discharge current is maximum. This work attempts to answer why there is an optimal value of the magnetic field through simulation. For the numerical solution of the Penning gas discharge problem model based on 2D/3D electrostatic Particle-In-Cell (PIC) method using structured rectangular grids and implemented in the VSim [2] software package. To simulate the kinetic processes in a gas-discharge plasma, the Monte-Carlo collision (MCC) method was used.

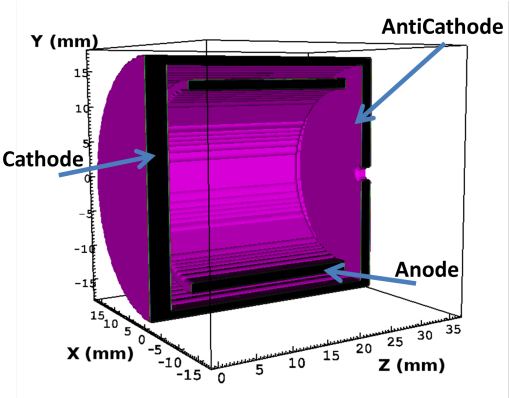

Figure 1: *Schematic view of the Penning gas discharge*

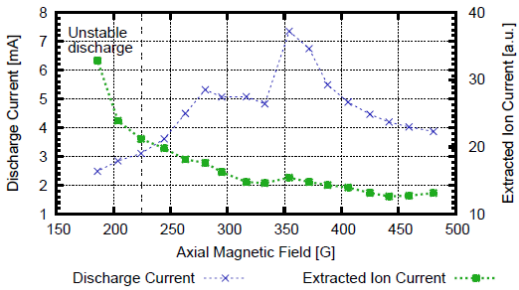

Figure 2: *Experimental current for different magnetic field (figure is borrowed from [1])*

The electron temperature $T_e \sim 10 \div 20\ eV$ should be expected in the Penning discharge, with an electron concentration of about $n_e \sim 2 \cdot 10^{16}\ m^3$. We can estimate: Debye radius (λ_D), electron

plasma frequency (ω_{pe}), electron cyclotron frequency (ω_{ce}). These values impose a limit on the size of the grids and the time step for the PIC-MCC method:

– Max cell size: $\Delta x_{max} < 3.4 \cdot \lambda_D = 3.4 \cdot 7433 \cdot \sqrt{\frac{T_e[eV]}{n_e[m^{-3}]}} \sim 0.57mm$

– Max time step for electron plasma frequency: $\Delta t_{max} < \frac{0.2}{\omega_{pe}} = \frac{0.2}{5.64 \cdot 10^4 \sqrt{n_e[cm^{-3}]}} \sim 25ps$

– Max time step for electron cyclotron frequency: $\Delta t_{max} < \frac{0.2}{\omega_{ce}} = \frac{0.2}{1.76 \cdot 10^7 \cdot B[G]} \sim 23ps$

For 2D calculations, the cell size was 0.25 *mm*. 3D calculations are very laborious and time consuming. Therefore, the cell size for 3D calculations was 0.50 *mm*, 0.33 *mm* and 0.25 *mm*. For the all numerical simulations time step was 10 *ps*.

The main elementary processes accounted for in the study were:

– elastic electron scattering on H_2 molecules ($e^- + H_2 \rightarrow e^- + H_2$) [3]

– ionization of H_2 molecules by electrons ($e^- + H_2 \rightarrow H_2^+ + 2e^-$) [3]

– H_2^+ charge exchange on H_2 molecules ($H_2^+ + H_2 \rightarrow H_2 + H_2^+$) [4]

– H_2^+ momentum exchange on H_2 molecules ($H_2^+ + H_2 \rightarrow H_2^+ + H_2$) [5]

– impact ionization of H_2 molecules by H_2^+ ($H_2^+ + H_2 \rightarrow H_2^+ + H_2^+ + e^-$) [6]

The distribution of fields, as well as the concentration of charged particles for 3D, will be represented as a projection of these fields on the XY and ZY plane in the some time step. Moreover, these planes (XY and ZY) are in the middle of the Penning discharge. This is necessary to image the disturbance of axial symmetry.

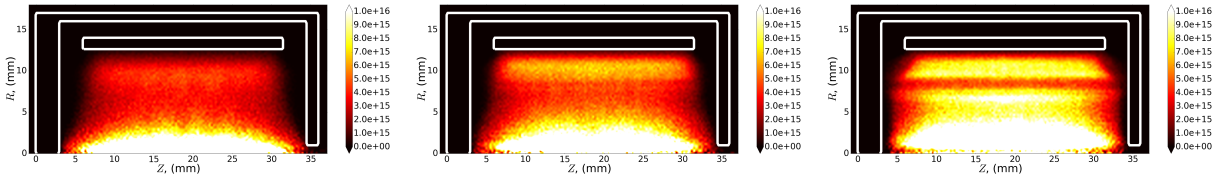

(a) *B=300G* (b) *B=400G* (c) *B=500G*

Figure 3: *Electrons density distribution in 2D simulation. Units for legend: [e^- in m^3].*

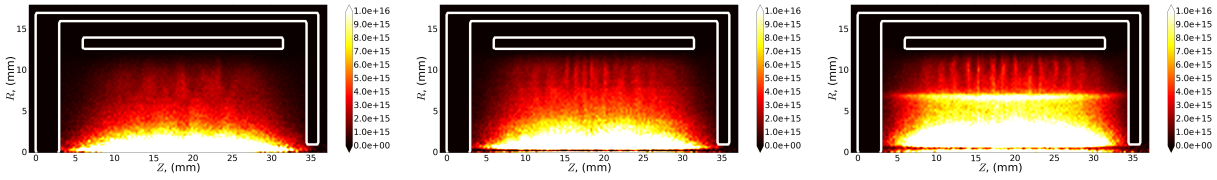

(a) *B=300G* (b) *B=400G* (c) *B=500G*

Figure 4: *Molecurlar ions density distribution in 2D simulation. Units for legend: [H_2^+ in m^3].*

The electrons densities distributions are presented on the figures 3, 5 for 2D/3D case, respectively. For 2D case two peaks are observed in the distribution of the electron density. The main

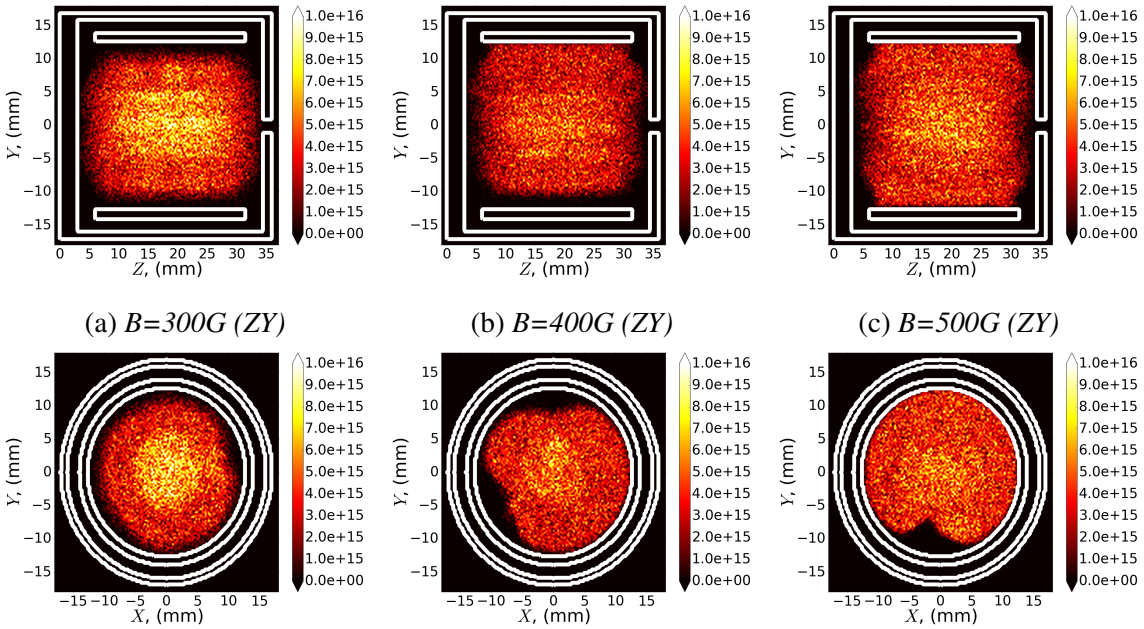

(a) *B=300G (ZY)* (b) *B=400G (ZY)* (c) *B=500G (ZY)*

(d) *B=300G (XY)* (e) *B=400G (XY)* (f) *B=500G (XY)*

Figure 5: *Electrons density distribution in 3D simulation. Units for legend: [e^- in m^3]. Project to ZY/XY.*

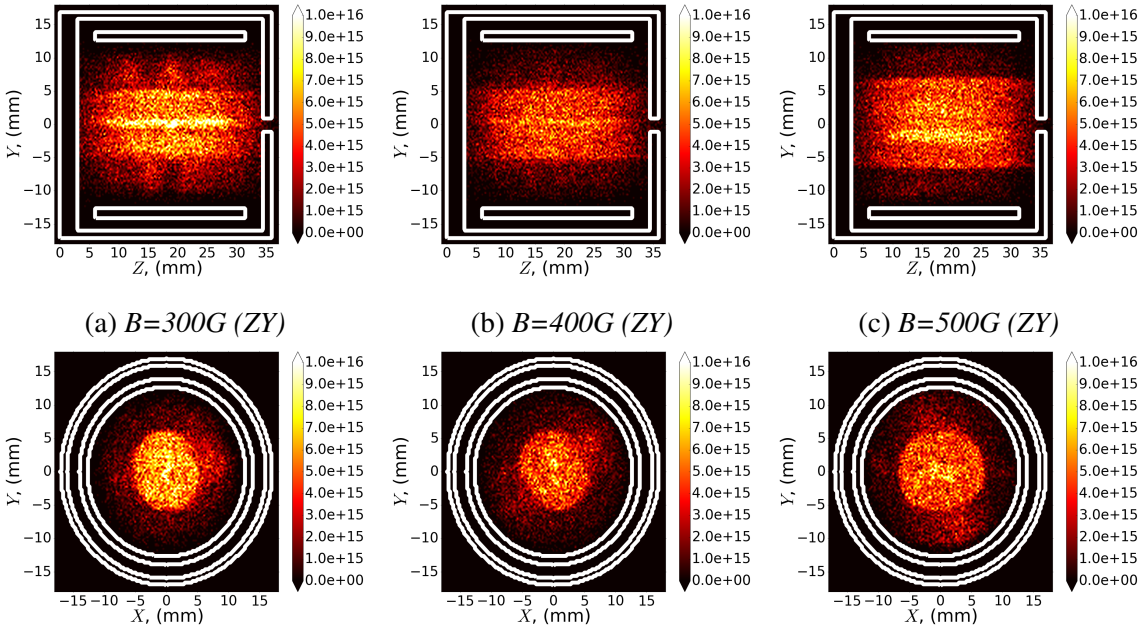

(a) *B=300G (ZY)* (b) *B=400G (ZY)* (c) *B=500G (ZY)*

(d) *B=300G (XY)* (e) *B=400G (XY)* (f) *B=500G (XY)*

Figure 6: *Ions distribution in 3D simulation. Units for legend: [H_2^+ in m^3]. Project to ZY/XY.*

peak is located near the axis of symmetry. A weaker second peak is observed in the near-anode region. For 3D case axial symmetry breaking is observed for the electron concentration distribution. At the same time, this distribution rotates around the axis of symmetry in time, preserving its structure.

The molecular ion densities distributions are presented on the figures 4, 6 for 2D/3D case, respectively. For 2D case the distribution of H_2^+ reaches the maximum near the axis of symmetry and then falls to the anode. The region occupied by molecular ions increases with increasing magnetic field. But this area is limited. For 3D case main part of molecular ions is concentrated in a cylinder with a radius of 5-6 *mm*. The distribution of the ions in this cylinder is not uniform and fluctuates in time. The spokes are observed in the distribution of molecular ions. In time, these spokes rotate.

The experiment [1] show that there exists I_{max} and corresponding B_{max} after which further increase in B leads to decrease in I. Our calculations showed that a similar behavior of the discharge current is observed in the simulation (see figure 7). Such a behavior of the discharge current from the magnetic field is due to the disturbance of the axial symmetry of the the distribution of electrons and ions (see figure 3, 5). Moreover, the disturbance of the axial symmetry of the electrons density is observed for a magnetic field above 300-350 *G*, which is in good agreement with experiment [1] (see figure 7). Also, if axial symmetry is disturbance, electron density form stable formations that rotate around the axis in time. The difference for discharge current in 3D modeling for different mesh sizes is observed. This may be due to the fact that the coarse mesh does not reproduce the field gradients well.

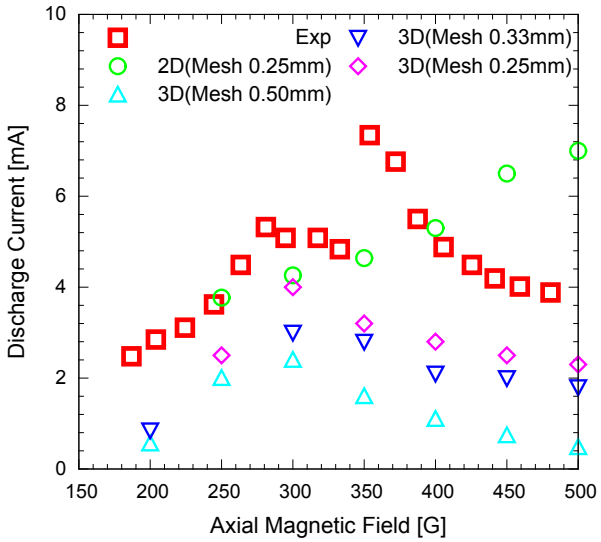

Figure 7: *Comparison of experimental and numerical data*

References

[1] A.V. Sy, Advanced Penning-type source development and passive beam focusing techniques for an associated particle imaging neutron generator with enhanced spatial resolution, Berkley: University of California, 2013

[2] C. Nieter, J.R. Cary, VORPAL: a versatile plasma simulation code, Journal of Computational Physics **196**, 2004

[3] S.J. Buckman, A.V. Phelps, JILA Information Center Report 27, University of Colorado, 1985

[4] C.F. Barnet, Oak Ridge National Laboratory, Report ORNL-6086, 1990

[5] P.S. Krstic, D.R. Schultz, Elastic and Related Transport Cross Sections for Collisions, 1998

[6] R.K. Janev, W.D. Langer, K.Jr. Evans, D.E. Post, Elementary Processes in Hydrogen-Helium Plasmas, 1987